IL NUOVO CIMENTO Vol. 24 C, N. 4-5 Luglio-Ottobre 2001

High energy cosmic rays in the low stratosphere and extrapolation above LHC energies(*)

J. N. Capdevielle(1), F. Cohen(1), I. Kurp(2), C. Le Gall(1)
B. Szabelska(2) and J. Szabelski(2)

(1) *PCC, Collège de France - 11 Pl. M. Berthelot, 75231 Paris Cedex 05, France*
(2) *The Andrzej Sołtan Institute for Nuclear Studies - 90-950 Łódź 1, Box 447, Poland*

(ricevuto l'8 Novembre 2000; approvato il 12 Febbraio 2001)

Summary. — We review the data obtained with the emulsion chambers boarded on Concorde for the events collected above 10^6 GeV and their specific properties (large multiplicities, multiclusters, coplanar emission): the main features are compared to the expectation of our HDPM2 Monte Carlo collision generator. This multiproduction event generator has been adjusted and tuned, according to the pseudo-rapidity distributions recently observed at $\sqrt{s} = 630$ GeV, as well as to previous Fermi-lab results at $\sqrt{s} = 1800$ GeV: an increase of the total inelasticity (0.72 for NSD component) near the knee region and a more important violation than usually expected for Feynman's scaling in forward region are observed. In such cirumstance, we have simulated large and giant air showers taking into account, in addition, new processes, such as diquark breaking, up to energies exceeding 10^{20} eV for P.AUGER and EUSO experiments.

PACS 13.85.Tp – Cosmic-ray interactions.
PACS 96.40.De – Composition, energy spectra, and interactions.
PACS 96.40.Pq – Extensive air showers.
PACS 01.30.Cc – Conference proceedings.

1. – The French-Japanese emulsion chamber exposures on the Concorde

Regular supersonic atlantic flights provide one "plateau exposure" of more than 2 hours. The same X-ray emulsion chamber carried one hundred times above the Atlantic is then exposed during 200 hours at least at an average altitude of 17 km. This corresponds, as indicated by the Concorde flight curve to an atmospheric depth of 100–105 g cm^{-2}. During the last 20 years, 8 emulsion chambers have been flown on the Concorde for different measurements, very high energy jets, stratospheric γ-ray families,

(*) Paper presented at the Chacaltaya Meeting on Cosmic Ray Physics, La Paz, Bolivia, July 23-27, 2000.

Table I. – *Some remarkable events recorded during Concorde flights.*

Event	ΣE_γ(TeV)	n_γ	$n_{\rm ch}$	Vertex
JFa1	18	4	26	producer
JF1af1	260	150	-	cabin wall
JF2af1	1586	211	-	100 m above
JF3.1	55	-	24	producer
JF3.2	51	-	54	producer
JF5.1	138	18	-	5 km

γ-ray flux [7, 1-3], gamma-ray energy spectrum in the interval 1–50 TeV, hyperstrange baryonic matter [4] and more recently emulsions for dosimetry (neutrons between 1 and 10 MeV). All the detectors, but the last one, were enough thick to measure, at least, the energy of secondary γ-rays up to 1000 TeV, allowing to initiate the collection of information on multiproduction in the energy range between the limit of the present colliders and the LHC. Those events (3 of them are above 10^6 GeV) are listed in table I.

The event JF1af1 resulted from a collision generated in cabin wall, about 3 m above the chamber and this circumstance was providential to build the rapidity distribution of the 150 γ's of energy exceeding 200 GeV. The characteristics of this event, high multiplicity, large transverse momentum suggest a classification in the nonsingle diffractive component with high z as expected from the negative binomial distribution. However, the multicluster structure and a pair of sharp spikes in the rapidity distribution require more simulations in 3 directions (fluctuations for individual events and random accumulation of secondaries by pure chance, Alpha primary and QGP). At larger energy, around 10^7 GeV, one impressive stratospheric family was collected; the probability to observe such energy with a so small time of exposure (area 40 cm $\times$ 50 cm for each chamber) is reduced and can be only compensated by a wide solid angle. This event was effectively very inclined with a zenith angle of 52°.

2. – The coplanar event of 10^7 GeV

The 211 γ's (above 200 GeV) of this event were identified with their respective coordinates and energies; the analysis was then focused on the typical multicluster structure and the planarity, ascertained by naked eye on the X-ray film, was confirmed, suggesting a multijet structure [3]. It is interesting to compare the event seen by naked eye from the picture of the X-ray film (fig. 1) and an event simulated at the same energy showing also an alignement obtained by pure chance from coincidence of favourable geometric and nuclear conditions. The similarity of the clusters (gammas above 10 TeV are plotted) with those of fig. 1 is especially interesting. Tracing back the genetics of this event, it belongs to the normal NSD multiple production with high multiplicity. The first collision occurred at an altitude of 24 km and the regression coefficient of the 32 gammas (above 10 TeV) is 0.968 with a total energy deposited of 815 TeV. The main features generating the alignement are here:

– high multiplicity,

– important zenith angle.

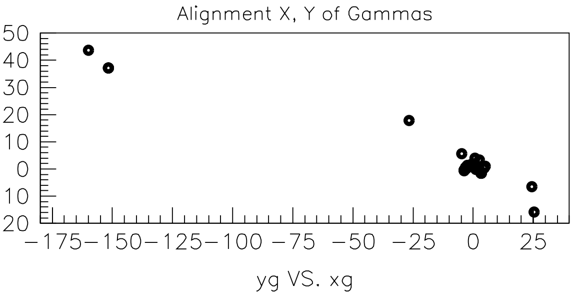

Fig. 1. – Coplanar emission visible in the event JF2af2 from the X-ray film. Several points with minor separations (bremsstrahlung or pair creation near the chamber) are superposed.

Both circumstances combine as follows: the probability to get a large transverse momentum is enhanced in high-multiplicity events and this large p_{t} can be devoted to a high energy gamma. This emission can be close, as here, to the vertical plane. The rest of the cluster is displaced in the opposite direction (p_{t} conservation and the maximal separation between gamma's appear in the horizontal plane (the emulsion or X sheets) with a characteristic gap visible in fig. 1 and in some events of Pamir). On our sample of 100 events, we have counted 2% of events with $r \geq 0.95$, 6% events with $r \geq 0.9$, 10% and 18% with r exceeding respectively 0.8 and 0.7. The combination of a large transverse momentum generated in the vertical plane (or in the neighbourhood) for an energetic secondary at 1st collision can be at the origin of the alignments observed in emulsion chambers. In that case the coplanar emission appears near 10^7 GeV where the ratio primary energy-energy threshold of the chamber is the most favourable. More simulations will be needed to confirm the increase of the probability of alignment observation at large zenith angle with a characterictic gap. The zenith angle distribution of coplanar events, associated to the frequency *versus* observed energy are probably the best criteria to understand if we have here a pure geometrical high-multiplicity fluctuation in the NSD component artefact or if this is a footprint of new physics.

3. – Extrapolation at ultrahigh energies

A special set of simulations has been carried out with the same zenith angle as for JF2af2 of 52° for 100 events. This was done with the model HDPM2 taking into account recent features of collider physics such as p_{t} *versus* central rapidity density (UA1-MIMI exp.) and recent results of Fermi-lab for pseudorapidity up to 5.5 [5]. The pseudo-rapidity distributions obtained with HDPM2 for 2000 collisions NSD are shown in fig. 2 [6].

As it was not possible to scan each individual event simulated, it was requested to calculate the linear regression line from the coordinates of the gammas and to plot only the events with a regression coefficient larger than 0.9. The event no. 47 of this serial selected by this method shows a nice alignment of 32 gamma's. As it can be ascertained, there are not very large differences between the HDPM2 and the QGS-jet model at collider energy. The extrapolations at higher energy can be different according to the parton distribution function assumed and there are several sets of parameters available. Another difficulty in the extrapolation can come from modifications generating wider amplitudes such as the mechanism of diquark breaking. Such effect can suppress the

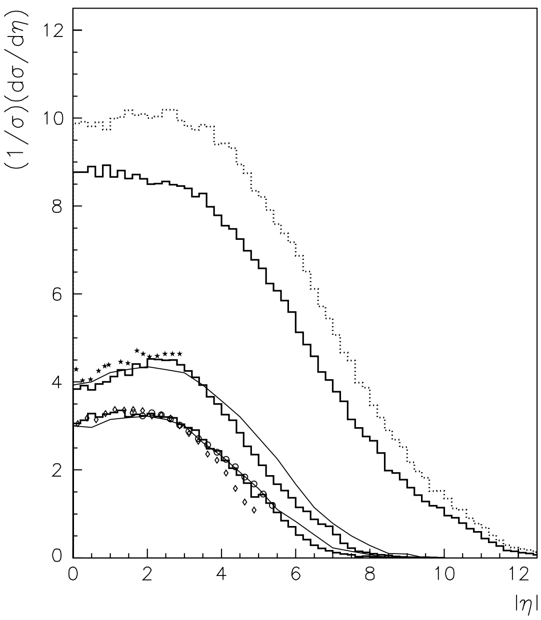

Fig. 2. – Pseudo-rapidity distributions with HDPM2.

leading-particle effect, classical for hadronic cascades if we consider that the valence diquark of the projectile is broken: the recombination of the diquark with one valence quark is impossible and a leading proton cannot emerge. We estimate that in such circumstance the maximum depth of EAS will be shifted systematically at higher altitude by 50 g cm^{-2} and this mechanism could help the understanding of a more realistic mass composition above the knee.

4. – Topological problems in giant EAS

Other difficulties may occur independently of the interaction model in the topological approach of the observables used to estimate the primary energy, for instance the profile of the lateral distribution assumed and the core localization. We propose instead of NKG and other Euler beta-functions, the employment of the Gaussian hypergeometric formalism giving also normalization and better skewness, under the form

$$f(x) = g(s)x^{s-a}(x+1)^{s-b}(1+dx)^{-c}\,, \tag{1}$$

which has the advantage (for values of parameters respecting the conditions of convergence $s-a+2>0$ and $c-2s+b-2>0$) to be exactly normalized in terms of Gaussian hypergeometric function $F_{\mathrm{HG}} = F(c, s-a+2, c+b-s; 1-d)$ by

$$g(s) = \frac{\Gamma(c+b-s)}{2\pi\Gamma(s-a+2)\Gamma(c-2s+b+a-2)F_{\mathrm{HG}}}\,. \tag{2}$$

TABLE II. – *Best parameters to simulated* e^+e^-+ *muons (all charged) lateral distribution fit using JNC01 formula.*

	p10	p20	Fe10	Fe20
$\log_{10} N_e$	10.75	10.72	10.70	10.65
r_M	21.26	21.26	19.18	19.18
r_0	8785.	8785.	9536.	9536.
a	1.91	1.91	1.82	1.82
s	1.03	1.04	1.03	1.04
b	3.32	3.32	3.31	3.31
β	10.0	10.0	10.0	10.0
$\chi^2(50)$	$12.1{\cdot}10^6$	$19.5{\cdot}10^6$	$6.87{\cdot}10^6$	$10.4{\cdot}10^6$
$\chi^2_P(50)$	$12.2{\cdot}10^6$	$20.2{\cdot}10^6$	$6.94{\cdot}10^6$	$10.6{\cdot}10^6$
Ξ	2.61	1.77	5.20	1.95

TABLE III. – *Columns a present total number of charged particles* N_e *in* 10^{10}, *columns b the ratios* E_0/N_e *in* GeV *(*$E_0 = 10^{11}$ GeV*) and columns c the ratios* $\varrho(600)/N_e$ *in* 10^{-8} *particles/m*^{2}. $m(600) = \frac{\mathrm{d}(\log\ \varrho)}{\mathrm{d}(\log\ r)}$ *at* 600 *m.*

	proton 10°			proton 20°			iron 10°			iron 20°		
$\varrho(600)$	290 m^{-2}			318 m^{-2}			369 m^{-2}			356 m^{-2}		
$E_0/\varrho(600)$ (GeV m^2)	$3.4 \cdot 10^8$			$3.1 \cdot 10^8$			$2.7 \cdot 10^8$			$2.8 \cdot 10^8$		
$m(600)$	–3.9			–3.6			–3.6			–4.0		
fit	1a	1b	1c	2a	2b	2c	3a	3b	3c	4a	4b	4c
Yakutsk	1.8	5.6	1.6	1.7	5.9	1.9	2.3	4.3	1.6	1.9	5.3	1.8
Linsley's	8.2	1.2	0.3	8.0	1.3	0.3	10.5	0.9	0.3	8.9	1.1	0.4
AGASA #1	2.4	4.2	1.2	2.6	3.8	1.2	3.1	3.2	1.1	2.9	3.4	1.2
AGASA #2	3.3	3.0	0.8	3.6	2.8	0.8	4.2	2.4	0.8	4.0	2.5	0.8
this work	5.6	1.8	0.5	5.6	1.9	0.6	5.1	2.0	0.7	4.5	2.2	0.7

The empirical distributions, such as AGASA function [8], as underlined by Vishwanath [9] enters in the category of hypergeometric Gaussian functions [10].

The value used in AGASA function for the coefficient C_e is just an approximation; the exact value is

$$C_e = \frac{\Gamma(\beta+\eta-\alpha)}{2\pi\Gamma(2-\alpha)\Gamma(\beta+\eta-2)}\,\frac{1}{F_{\mathrm{HG}}}\,.$$

The hypergeometric Gaussian function can be easily calculated from the hypergeometric series. This equation is equivalent to our version (3) containing the age parameter s with the relations between respective coefficients: $x = \frac{r}{r_{\mathrm{M}}}$, $d = \frac{r_{\mathrm{M}}}{r_0}$, $s = 1.03$, $\alpha = a - s$, $\eta = b - s + \alpha$. (The value of s is taken from the longitudinal development simulated.) We

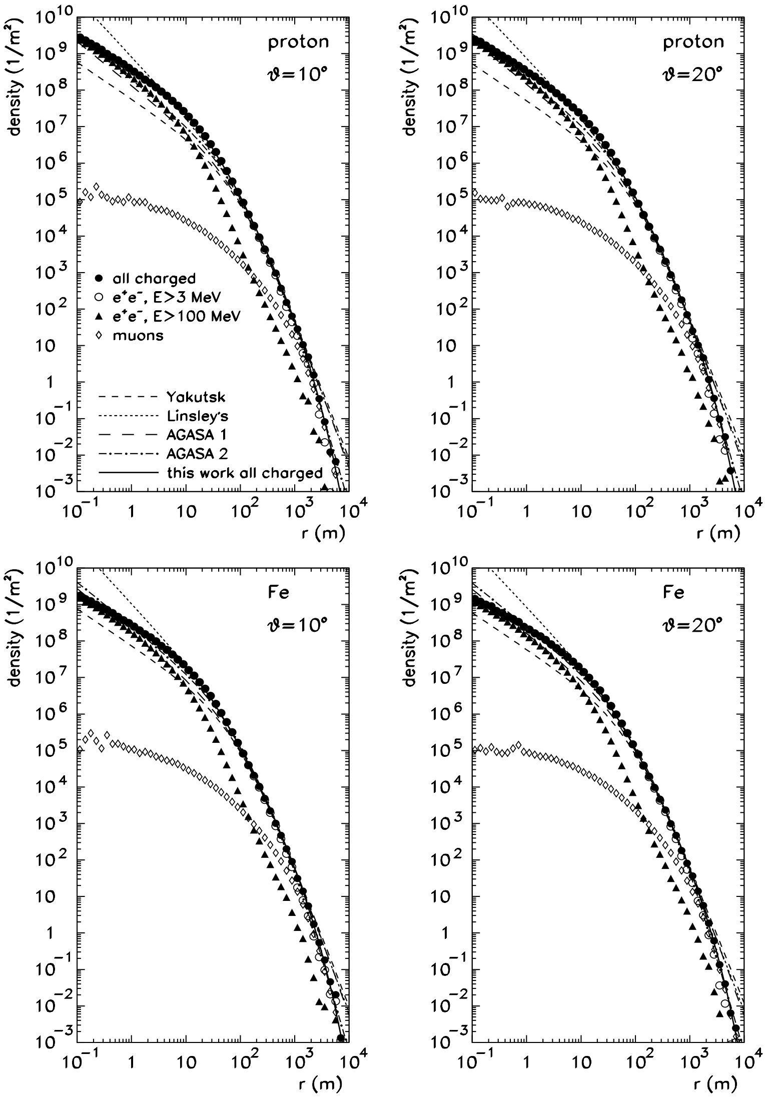

Fig. 3. – Fits to all charged particles lateral distribution from simulations (average from 10 EAS). Primary particle energy 10^{11} GeV. Lines are normalized to $\varrho(600\ \text{m})$.

have adjusted with MINUIT the parameters of our hypergeometric function (table II) to the average lateral distributions (set JNC01 for charged, JNC02 for electrons) of 10 showers at 10^{20} eV simulated with CORSIKA (QGSJET model), as shown in fig. 3.

In each case, the adjustment has been performed with 50 points from the simulation distributed from 0.1 m up to 10 km from the axis position for charged particles (muons and electrons) as shown in fig. 3. The advantages of JNC01 formula can be seen in fig. 3 and in table III. The major part of the particles is contained inside 200 m from the axis and only the skewness of the hypergeometric function allows a reliable relation between size and density at 600 m. This method has been applied to the showers contained in the catalogues of Volcano Ranch and Yakutsk. The core position has been obtained by minimization with Minuit program between different formulas available for lateral densities written *versus* the coordinates X, Y as

$$\varrho(r) = \varrho(\sqrt{(X - X_c)^2 + (Y - Y_c)^2})\,, \tag{3}$$

where the core coordinates X_c and Y_c are taken as two additive parameters in the minimization. The adjustments are generally improved when compared to the original treatments, turning to lower sizes (in the case of Yakutsk formula) and better approximation of the density at 600 m.

5. – Conclusion

As pointed out in sect. **2** the coplanar emission might not be a new characteristic of multiproduction near 10^7 GeV. More calculations at mountain altitude are requested to check if similar circumstances can be extended to the events observed in the Pamir X-ray chamber experiment. The large multiplicities of secondaries in those events remain however a common feature which could explain the tolerable agreement of models like QGSJET with EAS data. The hypergeometric approach gives a better accuracy in the interpolation of densities at 600–1000 m, a more reliable estimation of the shower size (when the axis is in the array), a better axis localization and finally a more correct constraint of the primary energy.

* * *

JNC is indebted to the colleagues of the emulsion division in Tokyo ICR/INS who have performed the complete scanning of this work. This work has been partly supported (JNC and CLG) by INTAS contract 1339.

REFERENCES

[1] Capdevielle J. N. *et al.*, *Proceedings of the 16th ICRC (Kyoto)*, vol. **6** (1979), p. 324.
[2] Capdevielle J. N. *et al.*, *Proceedings of the 20th ICRC (Moscow)*, vol. **5** (1987), p. 182.
[3] Capdevielle J. N. *et al.*, *J. Phys. G*, **14** (1988) 503.
[4] Capdevielle J. N. *et al.*, *Proceedings of the 24th ICRC (Rome)*, vol. **1** (1995), p. 910.
[5] Capdevielle J. N. *et al.*, *Proceedings of the 26th ICRC (Salt Lake City)*, vol. **1** (1999), p. 111.
[6] Capdevielle J. N., Le Gall C. and Sanosyan K., *Astropart. Phys.*, **13** (2000) 259.
[7] Iwai J. *et al.*, *Nuovo Cimento A*, **69** (1982) 295.
[8] Nagano M. *et al.*, *J. Phys. G.*, **18** (1992) 423.
[9] Vishwanath P. R., *Proceedings of the 23rd ICRC (Calgary), Rapporteur Papers*, vol. **6** (1993), p. 384.
[10] Capdevielle J. N. and Procureur J., *Proceedings of the 18th ICRC (Bangalore)*, vol. **11** (1983), p. 307.